Journal of Instrumentation

PAPER • **OPEN ACCESS**

Complex field verification using a large area CMOS MAPS upstream in radiotherapy

To cite this article: J.L. Pritchard *et al* 2022 *JINST* **17** C08018

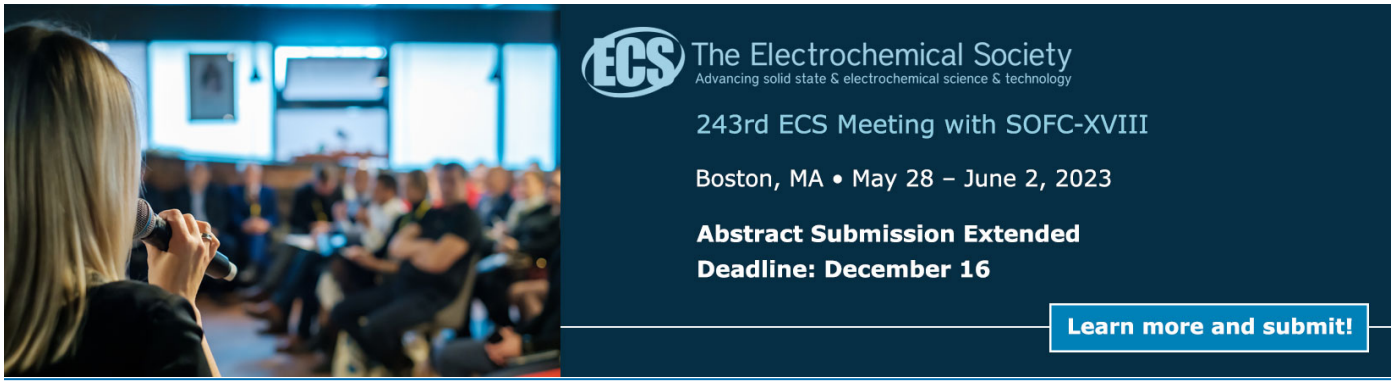

Published by IOP Publishing for Sissa Medialab

Received: *November 29, 2021*
Accepted: *June 8, 2022*
Published: *August 23, 2022*

12th International Conference on Position Sensitive Detectors
12–17 September, 2021
Birmingham, U.K.

Complex field verification using a large area CMOS MAPS upstream in radiotherapy

J.L. Pritchard,[a,*] **J.J. Velthuis,**[a,b,c] **L. Beck,**[a] **Y. Li,**[a] **C. De Sio,**[a] **L. Ballisat,**[a] **J. Duan,**[a] **Y. Shi**[a] **and R.P. Hugtenburg**[a,b,d]

[a] *School of Physics, University of Bristol, Bristol, BS8 1TL, United Kingdom*
[b] *Department of Medical Physics, Swansea University Medical School, Swansea, SA2 8QA, United Kingdom*
[c] *School of Nuclear Science and Technology, University of South China, Hengyang, 421001, People's Republic of China*
[d] *Department of Medical Physics and Clinical Engineering, Swansea Bay University Health Board, Swansea, SA2 8QA, United Kingdom*

E-mail: jordan.pritchard@bristol.ac.uk

Abstract: A multileaf collimator (MLC) is an integral component in modern radiotherapy machines as it dynamically shapes the photon field used for patient treatment. Currently, the MLC leaves which collimate the treatment field are mechanically calibrated to ±1 mm every 3 months and during pre-treatment calibration are calibrated to the mechanically set leaf positions. Leaf drift can occur between calibration dates and hence exceed the ±1 mm tolerance. Pre-treatment verification, increases LINAC usage time so is seldom performed for each individual patient treatment, but instead for an acceptable sample of patients and/or treatment fractions. Independent real-time treatment verification is therefore desirable. We are developing a large area CMOS MAPS upstream of the patient to monitor MLC leaf positions for real-time treatment verification. CMOS MAPS are radiation hard for photon and electron irradiation, have high readout speeds and low attenuation which makes them an ideal upstream radiation detector for radiotherapy. Previously, we reported on leaf position reconstruction for single leaves using the Lassena, a 12 × 14 cm^2, three side buttable MAPS suitable for clinical deployment. Sobel operator based methods were used for edge reconstruction. It was shown that the correspondence between reconstructed and set leaf position was excellent and resolutions ranged between 60.6 ± 8 and 109 ± 12 µm for a single central leaf with leaf extensions ranging from 1 to 35 mm using 0.3 sec of treatment beam time at 400 MU/min. Here, we report on leaf edge reconstruction using updated methods for complex leaf

*Corresponding author.

https://doi.org/10.1088/1748-0221/17/08/C08018

configurations, as occur in clinical use. Results show that leaf positions can be reconstructed with resolutions of 62 ± 6 µm for single leaves and 86 ± 16 µm for adjacent leaves at the isocenter using 0.15 sec at 400 MU/min of treatment beam. These resolutions are significantly better than current calibration standards.

KEYWORDS: Radiotherapy concepts; Solid state detectors; X-ray detectors; Image reconstruction in medical imaging

2022 JINST 17 C08018

Contents

1 Introduction

A multileaf collimator (MLC) is an integral component in modern radiotherapy machines. Their primary function is to (dynamically) shape the photon beam produced by the linear accelerator (LINAC) which is used for patient treatment. It is of fundamental importance that malignant tissue is precisely targeted and healthy tissue is minimally irradiated. This maximises the probability of patient cure and minimises the probability of secondary cancers occurring. The precision of advanced therapies is largely dependent upon an MLC's ability to precisely collimate the profile of the MV photon beam. Inside the MLC are two opposing rows of 40–120 tungsten leaves which move independently of each other. It is standard practise to calibrate them to a tolerance of ±1 mm every 3 months. Leaf drift can occur between calibrations and hence the ±1 mm tolerance can be exceeded. To maintain total dose errors below 2% for complex treatments, the verification tolerance should be set to a higher standard of ±0.3 mm [1, 2]. Pre-treatment verification is time consuming. Real-time verification is therefore desirable. We are developing a large area CMOS MAPS system based on the Athena, a further development of the LASSENA [3], placed upstream of the patient to verify the treatment in real-time by measuring leaf positions [4–6] and dose [7]. The sensor measures 12×14 cm^2, with a 3T pixel architecture and 50 µm pixel pitch. It is 3-side buttable, hence a combined imaging area of 28 cm in one direction and any multiple of 12 cm in the other is achievable. A 2×2 configuration of Athenas can therefore monitor full treatment fields. The sensor can be back-thinned to well below 100 µm without loss of performance. When back-thinned, the beam attenuation is <1% and therefore clinically insignificant [8].

Previously, we reported on leaf position reconstruction for single leaves in a square field [4, 6, 9]. Figure 1 (left) shows a Gaussian-smoothed intensity profile measured with the Athena for an MLC leaf inserted from the right. For details see section 3. The leaf blocks the photon beam leading to an abrupt change in signal intensity. Interactions of the photon beam with parts of the radiotherapy machine and the air result in a diffuse cloud of electrons. There are not many electrons, but the efficiency of detecting an electron is nearly 100%. The combination of the photon and electron field results in an error-function like signal on top of a smooth but non-constant background. This can be clearly seen in figure 1, where five slices through the leaf are shown.

2022 JINST 17 C08018

For single leaves, a slice along a pixel row is analysed and using a Sobel filter the point with the highest gradient is found as the leaf edge for that slice. For single leaves, these points form a parabola along the leaf edge, see figure 2. After fitting, the extreme position of the parabola is extracted as the leaf position. It was shown that correspondence between reconstructed and set leaf position was excellent and resolutions ranged between 61 ± 8 and 109 ± 12 µm for a central single leaf with leaf extensions ranging from 1 to 35 mm using 0.3 sec of treatment beam time at 400 MU/min.

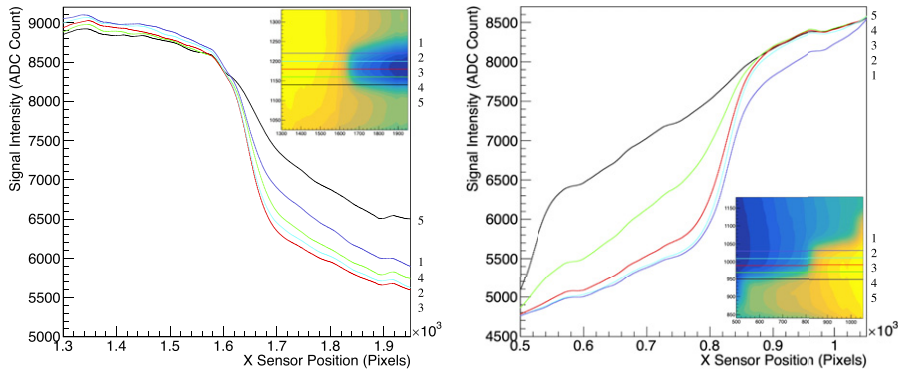

Figure 1. Two single data frames after Gaussian smearing and Sobel filtering for a single leaf (left) and an adjacent leaf (right).

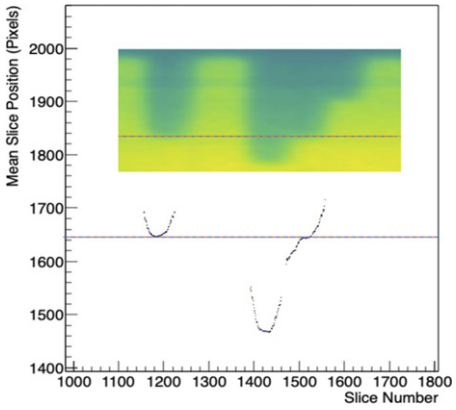

Figure 2. Points of highest gradient as a function of the slice number. On the left a single leaf is inserted from the top, while on the right a set of three MLC leaves with different extensions are inserted.

However, during clinical treatment, leaves are moved into complex configurations resulting in different scattering of the electrons and photons and thus changing the reconstructed leaf positions and resolutions. Here, we report on leaf edge reconstruction in complex leaf configurations, as occur in clinical use. When a leaf sticks out more than its neighbour, both photons and electrons

2022 JINST 17 C08018

are scattered off the leaf sides changing the intensity pattern measured with the Athena. The effect can be clearly seen in figure 1 (right), where a set of MLC leaves with different extensions are inserted from the left. The side away from the neighbour still produces the same signal shape, while the side close to the more extended leaf shows a different intensity pattern. As a result, the points with the highest gradient form a 3rd order polynomial instead of a parabola, see figure 2. Here results on the reconstructed leaf position resolutions for neighbouring leaves are reported.

2 Experimental setup

The Athena sensor was placed on a 160 leaf Elekta Agility LINAC treatment couch inside a light-tight environment. The detector was at 85 cm SSD. Dark data frames were measured and flat-field data was taken using an open $40 \times 40\,\mathrm{cm}^2$ photon flood field. A $40 \times 20\,\mathrm{cm}^2$ field was collimated using the *y*-jaw and a $14 \times 10\,\mathrm{cm}^2$ treatment field created using the MLC. This was done to increase electron and photon scatter components impinging the sensor. MLC leaves of 5 mm width at isocenter were extended from both leaf banks into the treatment field to create a range of leaf configurations. A 6 MV beam energy at 400 MU/min dose rate was selected and data frames were recorded at 34 fps. MLC leaves in the left bank were held in a fixed position, whilst leaves in the right bank were moved step-wise throughout the treatment field to create a series of data measurements.

3 Leaf position reconstruction methodology

Leaf positions are resolved following an updated version of the methods detailed in [6]. The signal of every pixel consists of a dark value, the pedestal and the beam-induced signal and noise. To determine the pedestal, the average signal for each pixel without beam was determined. The noise is determined as the standard deviation of the pixel output without beam. Pedestal subtraction and flat-field correction were applied as dark-current and gain-correction respectively. To reduce the random fluctuations between frames, five frames were averaged, reducing the effective frame rate to 6.8 fps. To reduce high-frequency pixel-to-pixel variation, images were smoothed using a Gaussian smearing with a radius of 31 pixels and a sigma of 7. As mentioned before, transitioning from the open field to the area shielded by the MLC leaf produces an S-curve at the field-leaf boundary. The leaf edge position is defined as the point of highest gradient. Single and adjacent leaf projections are fitted with a 2nd and 3rd order polynomial respectively and the fit turning point is used as the final leaf position. Plotting the reconstructed position as a function of set leaf position for single leaves and fitting with a straight line, as seen in figure 3 returns a gradient of 1.00 ± 0.01, showing the correct leaf positions are returned. The differences between reconstructed and set positions as a function of set position for single leaves are shown in figure 5 (left; black circles) and the residual distribution in figure 5 (right). Fitting the residual distribution with a Gaussian yields a resolution of 62 ± 6 µm.

2022 JINST 17 C08018

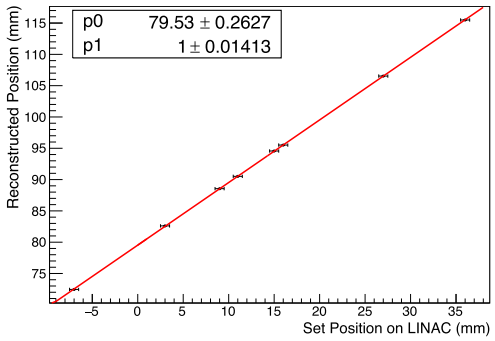

Figure 3. Reconstructed leaf position as a function of the set leaf position for single leaves. Excellent linearity is observed.

3.1 Adjacent leaves

The positions initially returned for the adjacent leaves are offset depending on the difference in leaf extension with their more extended neighbour. This is shown in figure 4, where the difference between reconstructed position and set position for adjacent leaves as a function of the separation distance between the adjacent leaf and its neighbour is shown. The initial and uncorrected reconstructed position for adjacent leaves is off-set and ranges between 400 and 1300 µm. This offset is caused by an accumulation of electron and photon scatter components at the tip of the adjacent leaves which are a function of separation distance between the measured (adjacent) leaf and its neighbour. A 3rd order polynomial is applied to parameterise the offset such that a correction to measured position can be applied as a function of neighbouring leaf position. After applying the correction, the adjacent leaves also return accurate positions. This can be seen in figure 5 (left; blue triangles). The residual distribution is shown in figure 5 (right). The resolution for the adjacent leaves is 86 ± 16 µm, which is worse than the resolution for single leaves but still well within the 300 µm range as required to provide accurate treatments.

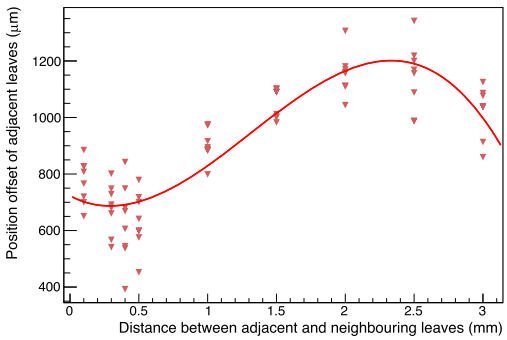

Figure 4. Difference between reconstructed position and set position for adjacent leaves as a function of the separation distance between the adjacent leaf and its neighbour. A 3rd order polynomial is used to parameterize the offset.

2022 JINST 17 C08018

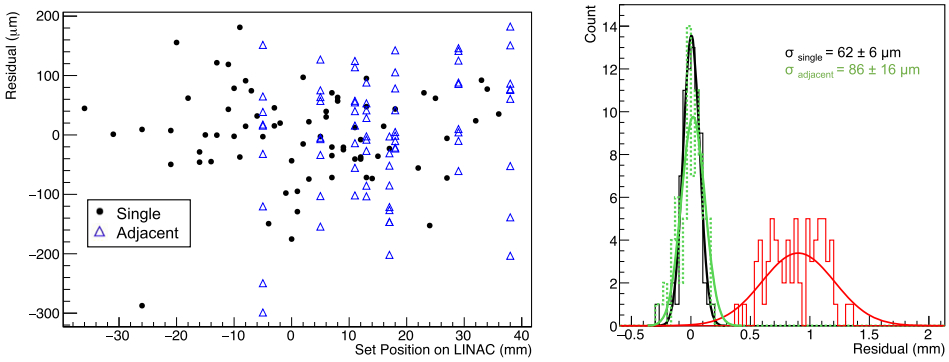

Figure 5. Difference between reconstructed and set position as a function of set position for single (black circles) and adjacent (blue triangles) leaves after adjacent leaf position correction. (b) Residual distribution for single (black), uncorrected (red) and corrected (green) adjacent leaves. The position resolution for adjacent leaves is worse than for single leaves, but both are well within the recommended strict guidelines of ±300 µm.

4 Conclusions

We are developing a CMOS MAPS-based real-time radiotherapy upstream treatment verification device. A key task of such a system is to monitor MLC leaf positions in real-time. The results presented here demonstrate that using the Athena sensor, a leaf position resolution of 86 ± 16 µm at isocenter is obtained for challenging leaf configurations as occur in clinical fields using 0.15 s of treatment data. These results are significantly better than the higher recommended MLC verification standard of ±0.3 mm. With this system, treatment errors could be detected instantaneously and treatment subsequently halted or amended, hence increasing treatment quality and patient safety.

Acknowledgments

The authors would like to thank Nordson for their advice and support.

References

[1] A. Agarwal et al., *Evaluating the dosimetric consequences of MLC leaf positioning errors in dynamic IMRT treatments, J. Radiother. Pract.* **18** (2019) 1.

[2] A. Rangel and P. Dunscombe, *Tolerances on MLC leaf position accuracy for IMRT delivery with a dynamic MLC, Med. Phys.* **36** (2009) 3304.

[3] N. Guerrini, R. Turchetta, G. Van Hoften, R. Henderson, G. McMullan and A.R. Faruqi, *A high frame rate, 16 million pixels, radiation hard CMOS sensor,* 2011 *JINST* **6** C03003.

[4] J. Velthuis, P.R. Hugtenburg, C. Hall, R. Page and P. Stevens, *Monitoring of a therapeutic X-ray beam using an active pixel sensor detector*, *Patent granted in EU on 04/04/2018*, EP2654895B1.

[5] J. Velthuis, P.R. Hugtenburg, C. Hall, R. Page and P. Stevens, *Upstream direct X-ray detection, U.S. patent no. 9517358*, U.S. Patent and Trademark Office, Washington, DC, U.S.A. (2016).

[6] J.L. Pritchard, J.J. Velthuis, L. Beck, C. De Sio and R.P. Hugtenburg, *High-resolution MLC leaf position measurements with a large area MAPS, IEEE Trans. Radiat. Plasma Med. Sci.* **5** (2020) 392.

2022 JINST 17 C08018

[7] L. Beck, J.J. Velthuis, R.F. Page, R.P. Hugtenburg, C. De Sio and J. Pritchard, *A novel approach to contamination suppression in transmission detectors for radiotherapy,* *IEEE Trans. Radiat. Plasma Med. Sci.* **4** (2020) 637.

[8] L. Beck, J.J. Velthuis, S. Fletcher, J.A. Haynes and R.F. Page, *Using a TRAPS upstream transmission detector to verify multileaf collimator positions during dynamic radiotherapy delivery,* *Appl. Radiat. Isot.* **156** (2020) 108951.

[9] C. De Sio, J.J. Velthuis, L. Beck, J.L. Pritchard and R.P. Hugtenburg, *r-Unet: leaf position reconstruction in upstream radiotherapy verification,* *IEEE Trans. Radiat. Plasma Med. Sci.* **5** (2021) 272.

2022 JINST 17 C08018